Normal Modes of Aluminum by Neutron Spectrometry*

B. N. BROCKHOUSE AND A. T. STEWART†

Physics Division, Atomic Energy of Canada Limited, Chalk River, Ontario, Canada

I. INTRODUCTION AND THEORY

THE theory of the scattering of neutrons by a crystal[1–5] indicates that the energy distribution of coherently scattered neutrons can be used to determine the frequency wave-number dispersion relation of the normal modes of the crystal in a very direct way. Interactions of the neutron with the crystal occur in which the neutron is scattered (a) elastically, (b) inelastically with the production or annihilation of a single quantum (phonon) of one normal mode—a one phonon process—or (c) inelastically with production and/or annihilation of a single quantum of each of several normal modes—a many-phonon process. The many phonon process is not readily interpretable and it is made unimportant by proper arrangement of experimental conditions.

For coherent scattering the elastic process is governed[1] by the Bragg law which can be written as

$$\begin{aligned} \mathbf{k}-\mathbf{k}' &= 2\pi\boldsymbol{\tau} \\ k^2 &= k'^2, \end{aligned} \tag{1}$$

where $\mathbf{k}$ and $\mathbf{k}'$ are the incoming and outgoing neutron propagation vectors (of magnitude $2\pi \times$ the neutron wave number) and $\boldsymbol{\tau}$ is a vector of the reciprocal lattice of the crystal.

The one-phonon process is governed by equations[2,3] which can be considered as the equations of conservation of momentum and of energy between the neutron, the phonon and the crystal as a whole, *viz.*,

$$\mathbf{k}-\mathbf{k}' = 2\pi\boldsymbol{\tau}-\mathbf{q}, \tag{2a}$$

$$E-E' = h\nu, \tag{2b}$$

where $E=\hbar^2k^2/2m$ and $E'=\hbar^2k'^2/2m$ are, respectively, the incoming and outgoing neutron energies, m is the mass of the neutron, and ν and $\mathbf{q}$ are the frequency and propagation vector of the normal mode to which the phonon belongs. The vector $\mathbf{q}$ ranges over one zone of reciprocal space. The relation between the frequency ν and propagation vector $\mathbf{q}$ of the normal modes is a fundamental property of the crystal, determined by its geometrical structure and the interatomic forces. This dispersion relation

$$\nu=\nu_j(\mathbf{q}), \tag{3}$$

where j identifies the branch of the vibrational spectrum, offers a direct approach to the determination of the atomic force constants in the crystal. For a crystal with one atom per unit cell j takes values from 1 to 3.

Many workers in different laboratories recognized that neutron inelastic scattering experiments, interpreted by Eqs. (2), offer a means of determining the frequency wave-number dispersion law [Eq. (3)] of the normal modes of a crystal. Monoenergetic neutrons are made incident on the crystal in some particular orientation and the energy distribution of the scattered neutrons is observed at some particular angle. The experimental conditions (angle of scattering, crystal orientation, temperature, etc.) are arranged so that the one-phonon process is the most important inelastic process. Neutron groups which satisfy Eqs. (2) should then be observed. The energy E' and propagation vector $\mathbf{k}'$ of these groups then define the frequency ν and propagation vector $\mathbf{q}$ of the normal modes with which the neutrons interacted. By repeated observation of energy distributions for different incident energies, angles of scattering, or orientations of the crystal, the $\nu(\mathbf{q})$ relation for the crystal can be built up. Experiments have demonstrated the existence of these neutron groups [6,7] and have shown clearly the dispersion of transverse modes propagating in the 111 direction in an aluminum crystal[8] and in other directions.[9]

The cross section for the one-phonon process is proportional to the square of the component of the polarization vector in the direction of the momentum transfer $\mathbf{k}-\mathbf{k}'$ [Eq. (4)]. Hence it appears that by repeated observation of the same normal mode under different experimental conditions it should be possible to measure the direction of polarization of the normal mode.

---

* Most of this work was presented at meetings of the Royal Society of Canada [Trans. Roy. Soc. Can. **III**, 50 (1956), papers 62, 63] and the American Crystallographic Association in June, 1956. The complete work was presented at the International Conference in Current Problems of Crystal Physics, Massachusetts Institute of Technology, July 1–5, 1957.

† Now at Physics Department, Dalhousie University, Halifax, Nova Scotia.

[1] G. C. Wick, Physik Z. **38**, 403, 689 (1937). I. Pomerantschuk, Physik. Z. Sowjetunion **13**, 65 (1938).

[2] R. Seegar and E. Teller, Phys. Rev. **62**, 37 (1942).

[3] R. Weinstock, Phys. Rev. **65**, 1 (1944).

[4] I. Waller and P. O. Froman, Arkiv Fysik **4**, 183 (1952).

[5] G. Placzek and L. Van Hove, Phys. Rev. **93**, 1207 (1954).

[6] B. N. Brockhouse, Trans. Roy. Soc. Can. **III**, **49** (1955), paper 118. Issued as AECL No. 221.

[7] Carter Muether, Hughes, and Palevsky, Bull. Am. Phys. Soc. Ser. II, **1**, 55 (1956).

[8] B. N. Brockhouse and A. T. Stewart, Phys. Rev. **100**, 756 (1955).

[9] We wish to thank Carter, Hughes, and Palevsky for a preprint of a paper [Phys. Rev. **106**, 1168 (1957)]. Their paper contains results similar to those given in our Fig. 9.

In this paper we present an extensive series of measurements on a single crystal of aluminum from which we have obtained the frequency wave-number dispersion relations for the 110 and 100 planes of the aluminum crystal, and some qualitative information about the polarization directions. Aluminum was selected as the first material for study because it has a simple structure (face-centered-cubic), lattice frequencies in a convenient range for this experiment, and excellent nuclear properties (small capture and incoherent scattering). In addition the elastic constants have been well measured,[10] and a study of the lattice frequencies by x-rays was known to be underway.[11]

The result of our measurements for the simple directions of the types 100, 110, and 111 are in fair agreement with dispersion relations obtained from x-ray intensity measurements by Walker,[11] and for the other directions are in fair agreement with the dispersion relations deduced by Walker from his measurements in the special directions. We have made calculations of dispersion relations for simple models using the Born lattice dynamics[12] and compared them with the measured dispersion curves and with the elastic constants. Even when the comparison is restricted to the transverse modes in the special directions relatively complex models are required to obtain a fit.

II. EXPERIMENTAL METHODS

The two different experimental systems will be described briefly. In one method the monoenergetic incident neutrons are obtained by Bragg reflection from a crystal and the energy distribution of the scattered neutrons analyzed by means of a crystal spectrometer. In the other method the monoenergetic incident neutrons are obtained by means of cold neutron filters and the energy distribution of the scattered neutrons analyzed by measuring their time of flight with a neutron chopper.

1. Specimens

The specimen aluminum crystals were cut from single crystal ingots grown in graphite crucibles by the Bridgman method from "superpure" aluminum. For two experiments designated A and B in Sec. III the specimen was a slab about $6\times2\frac{1}{4}\times1$ in. with the 111 axis normal to the large face and $01\bar{1}$ axis parallel to the $2\frac{1}{4}$-in. direction. For the other experiments, C to G, the specimen was a sphere of $2\frac{1}{2}$-in. diameter.

2. Crystal Spectrometer Method

A diagram of the apparatus is shown in Fig. 1. Monoenergetic neutrons were obtained by Bragg reflection from the 111 plane of an aluminum single crystal X_1. For most of the experiments the specimen crystal S was oriented with its $01\bar{1}$ axis normal to the plane of the spectrometers (paper). The angle of scattering (ϕ) and the orientation of the specimen crystal in the spectrometer plane was set so that Bragg reflection from some plane would occur. The angle ϕ was then fixed and the specimen crystal reoriented to some other angle ψ removed from the Bragg position (ψ_0). The energy distribution of the neutrons scattered under these conditions was obtained by means of the analyzing crystal spectrometer, which again used the 111 plane of an aluminum crystal X_2. A true background was obtained by turning the analyzing crystal (X_2) out of the Bragg position for alternate time intervals. This background was then subtracted point-by-point from the adjacent signal record. An intensity calibration of the analyzing spectrometer was obtained by comparing a theoretical Maxwellian spectrum with the measured energy distribution of the neutrons scattered from the interior of a block of paraffin.[13] When the intensities permitted an extra collimator was inserted at Cl in Fig. 1 to improve the resolution of the incoming beam.

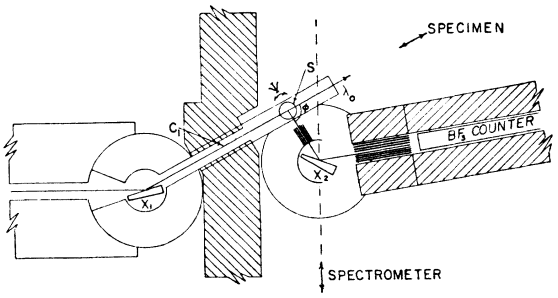

FIG. 1. Schematic drawing of crystal spectrometer apparatus.

Typical distributions are shown in Fig. 2(a) for an aluminum crystal in various orientations and for the vanadium standard. The vanadium pattern gives the resolution function at the incoming energy since the peak consists of incoherent elastic scattering.[14] From the pattern the resolution function at other energies can be inferred through approximate knowledge of the elements of the apparatus. The aluminum patterns show neutron groups whose energy depends on the orientation of the specimen crystal. The centers of these groups give the values of $\mathbf{k}'$ and E' required for application of Eqs. (2).

3. Filter-Chopper Method

The apparatus is shown schematically in Fig. 3. A neutron beam from the NRX reactor was passed through

[10] D. Lazarus, Phys. Rev. **76**, 545 (1949); P. M. Sutton, *ibid.* **91**, 816 (1953); T. R. Long and C. S. Smith, Office of Naval Research Technical Report (July, 1953), as quoted in references 11 and 19.

[11] C. B. Walker, Phys. Rev. **103**, 547 (1956).

[12] G. H. Begbie and M. Born, Proc. Roy. Soc. (London) **A188**, 179 (1946); M. Born and K. Huang, *Dynamical Theory of Crystal Lattices* (Oxford University Press, New York, 1954).

[13] Further details on the crystal spectrometer method will be found in "Structural dynamics of water by neutron spectrometry," B. N. Brockhouse, [Proceedings of the Varenna conference on the condensed state of simple systems, Nuovo cimento Suppl. See also Phys. Rev. **106**, 859 (1957)].

[14] B. N. Brockhouse, Can. J. Phys. **33**, 889 (1955).

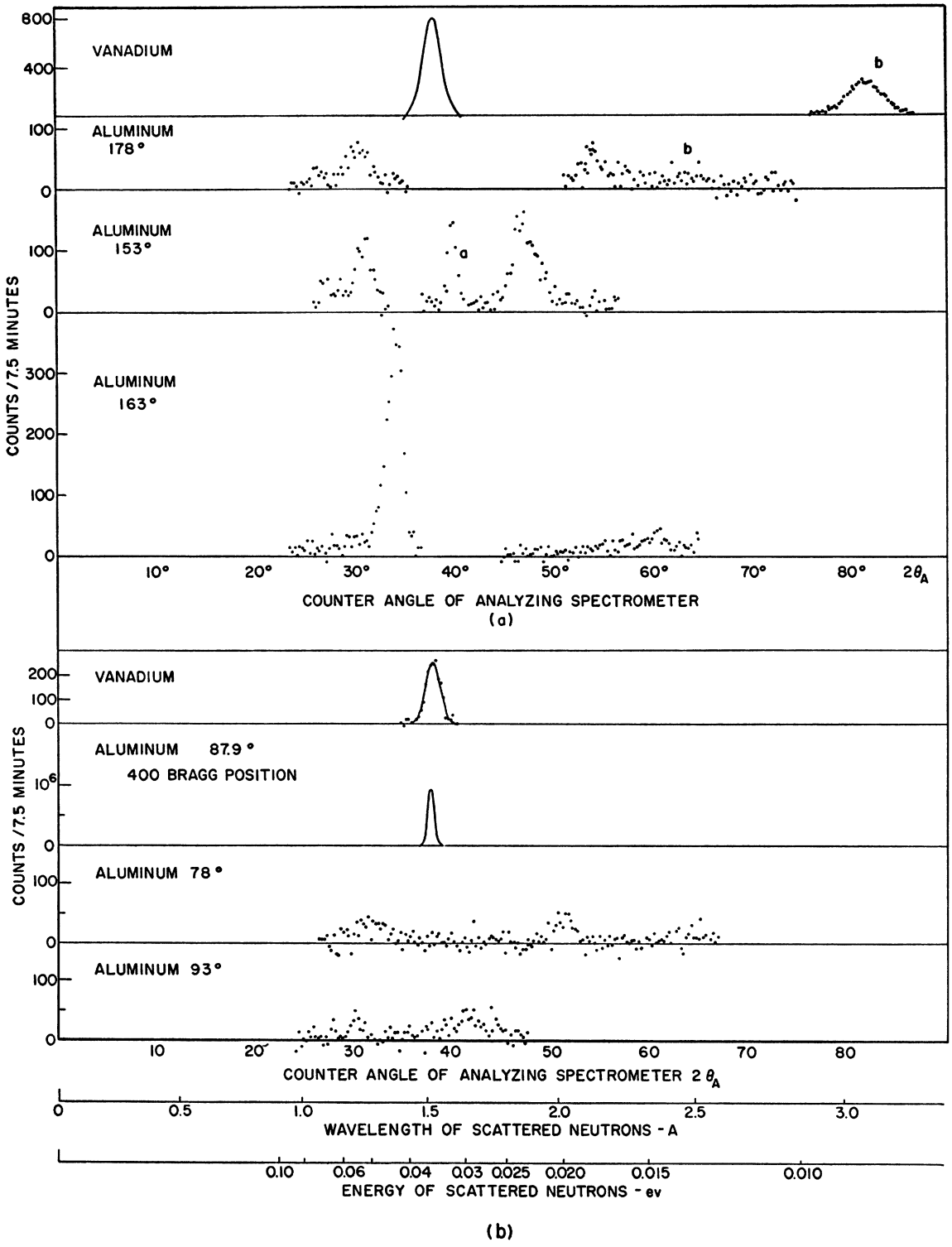

FIG. 2. Typical energy distributions for the crystal method. The counting rate is plotted as a function of the angle of the analyzing spectrometer for the vanadium standard and for the aluminum crystal in several different orientations, under two different resolutions. The group labeled (a) is believed to arise from Bragg scattering of second-order neutrons and those labeled (b) are groups viewed in the second order of the analyzing crystal. The resolution is indicated by the width of the vanadium groups.

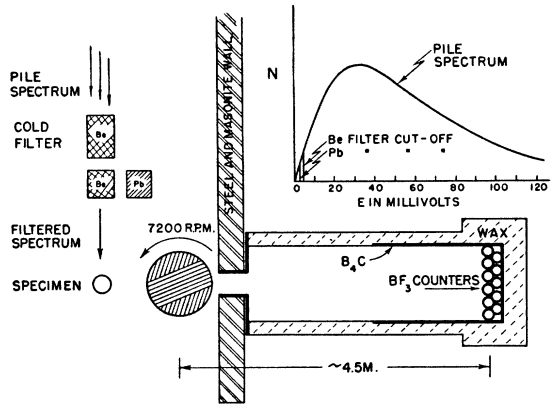

FIG. 3. Schematic drawing of filter-chopper apparatus.

a filter of beryllium metal thus removing by Bragg reflection neutrons whose wavelengths are shorter than 3.96 A. The filter was cooled by liquid nitrogen to increase the transmission of the desired long wavelength (cold) neutrons. Auxiliary filters of lead and beryllium were interposed in the cold neutron beam. These filters were matched so that they transmit equally (in the mean) neutrons whose wavelength is longer than 5.70 A. Neutrons between 3.96 A and 5.70 A were removed from the beam by the lead filter but not by the beryllium filter.

The beam of cold neutrons impinged on the specimen crystal whose orientation with respect to the apparatus was determined by Bragg reflection of contaminant short wavelength neutrons. The velocities of the neutrons scattered by the crystal through an angle of 90° were measured by means of a Fermi-type chopper and time-of-flight apparatus. The maximum angle of acceptance of the chopper was 6°. The chopper rotated at 7200 rpm producing 240 bursts of neutrons per second of maximum duration 140 μsec. The time to traverse the flight path of 4.45 meters was measured and the times displayed on a time sorter with 30 channels of approximately 120 μsec width.

Time-of-flight spectra of the scattered neutrons were observed with the auxiliary beryllium and lead filter alternately in the beam. Subtraction of the spectrum taken with the lead filter (Pb spectrum) from that with the beryllium filter (Be spectrum) gives the spectrum for incoming neutrons of between, 2.5 and 5.2×10^{-3} ev that is for a mean energy of 4.0×10^{-3} ev. The intensities were corrected by means of a calculated sensitivity curve for the instrument.

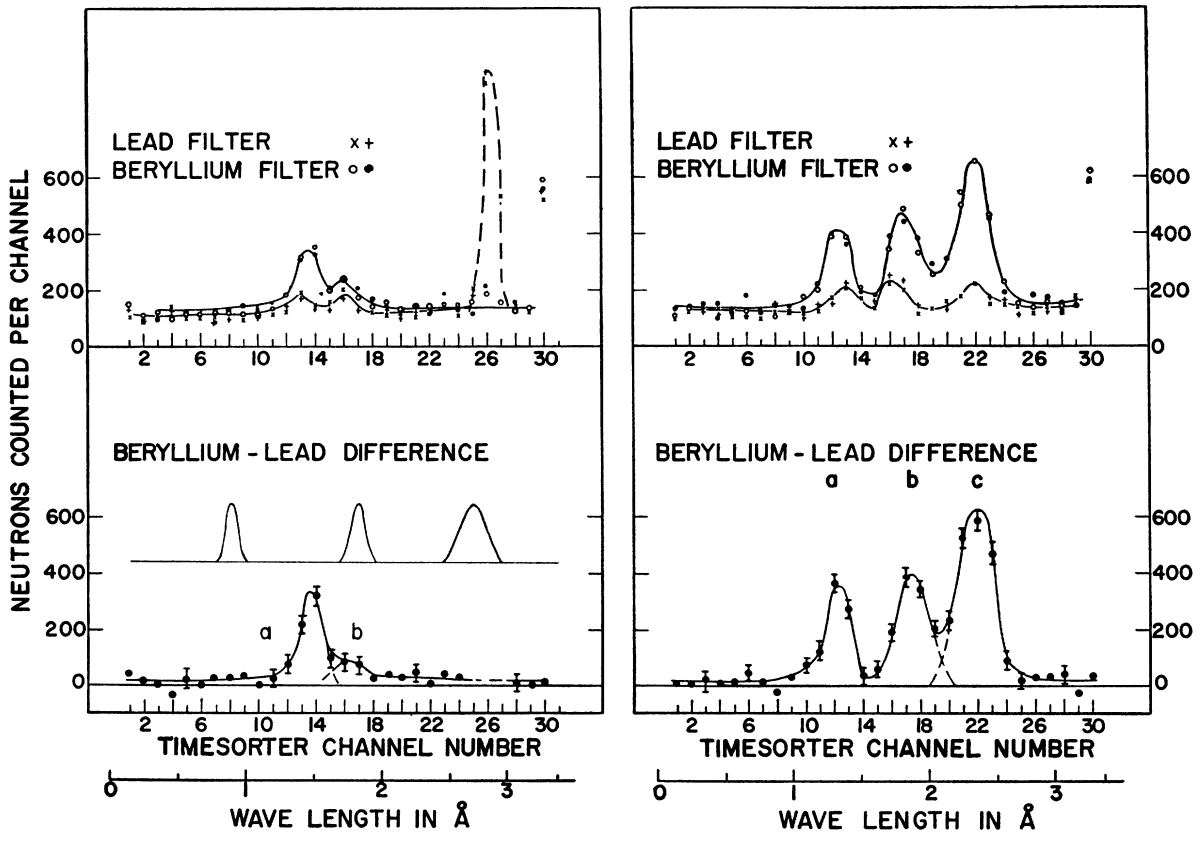

FIG. 4. Typical distributions in filter-chopper method. In the upper figures the counting rate is plotted as a function of the time channel number with beryllium and lead filters in the incoming beam. The lower figures show the beryllium-lead difference pattern.

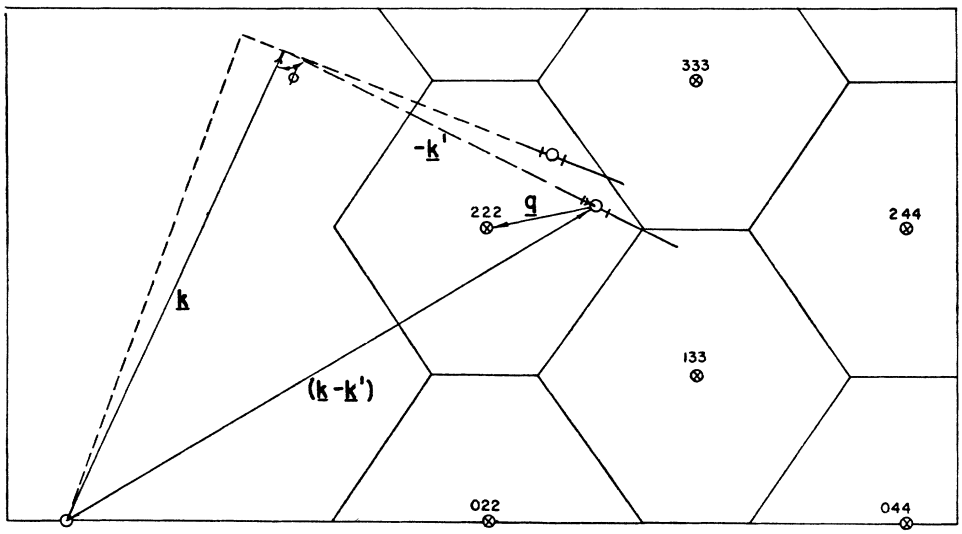

FIG. 5. The reciprocal lattice of aluminum in the $01\bar{1}$ plane with the system of zone boundaries. The vectors plotted represent Eq. (2a). The neutron groups shown are those obtained in experiment *B*.

Further details of the methods[15] are given elsewhere in this issue.[16]

Figure 4 shows typical distributions with the specimen aluminum sphere in two different orientations plotted as a function of the channel number, with an auxiliary wavelength scale. The patterns taken with the beryllium and lead auxiliary filters alternately in position are shown in the upper half of the figure. Two runs with each filter were taken and are shown in the figure. The differences between the sums of the patterns obtained with each of the two filters are shown in the lower half of the figure. The neutron groups are observed to be sharpened by the subtraction procedure, and in some cases an appreciable shift in their mean positions occurs. The left-hand lead pattern of Fig. 4 shows a remnant of one of the contaminant Bragg peaks which were used to align the crystal and to check the calibration of the wavelength scale. The calculated resolution width of the chopper and counter combination folded with the incident energy width is shown on the left-hand side of Fig. 4. The small number of channels into which any peak falls results in a further increase in the widths of the observed neutron groups.

The wavelength scale was checked by five measurements of the 200 or 220 Bragg reflection which gave an average of 0.98 ± 0.014 for the ratio of measured to calculated wavelength, assuming the angle of scattering to be accurately known. As the origin of this discrepancy, if real, was unknown, the calibration as determined from the flight path and time measurements was used.

[15] A somewhat similar apparatus without use of the subtraction procedure has been developed by Carter, Hughes, and Palevsky, references 7 and 9.

[16] A. T. Stewart and B. N. Brockhouse, Revs. Modern Phys. **30**, 250 (1958), following paper.

III. EXPERIMENTAL RESULTS

1. Scattering Curves

Several sets of experiments were performed under different conditions and will be described. In each case the centers of the neutron groups as measured were used to obtain $|\mathbf{k}'|=2\pi/\lambda'$ from which the vector $\mathbf{k}'$ could be deduced by knowledge of the angle of scattering and crystal orientations. The vectors $\mathbf{k}$ and $\mathbf{k}'$ are plotted on the reciprocal lattice diagram of the crystal and the vector $\mathbf{q}$ obtained by joining the tip of $\mathbf{k}'$ to the nearest reciprocal lattice point as shown in Fig. 5. Figures 6 to 9 show the results of the experiments which are described later. Where the full width at half-maximum of the observed neutron groups is greater than the diameter of the circle indicating the center of the group, it is shown as an error bar in the direction of $\mathbf{k}'$. Doubtful groups are indicated by means of dashed circles or bars. It is sometimes desirable to reflect the positions of the observed neutron groups into other sections of the reciprocal lattice by use of symmetry properties of the $\nu_j(q)$ relation. Such reflected groups are indicated by small filled circles. Relative intensities (corrected for the sensitivity of the instruments) are indicated by small numerals within the circles indicating the neutron groups.

The resolutions of the two experimental arrangements were estimated and are shown in some of the reciprocal lattice diagrams. In the crystal spectrometer apparatus the errors in the determination of $\mathbf{k}$ and $\mathbf{k}'$ are similar and were estimated from the collimator geometry and the mosaic of the monochromating and analyzing crystals. For the filter-chopper experiment the angular divergences are known from geometry and the spread in $|\mathbf{k}|$ from the Be and Pb cutoff wavelengths. The finite number of channels creates an additional uncertainty in $|\mathbf{k}'|$. In both Figs. 7 and 9 the outer lines of the resolution figures represent the estimated limits

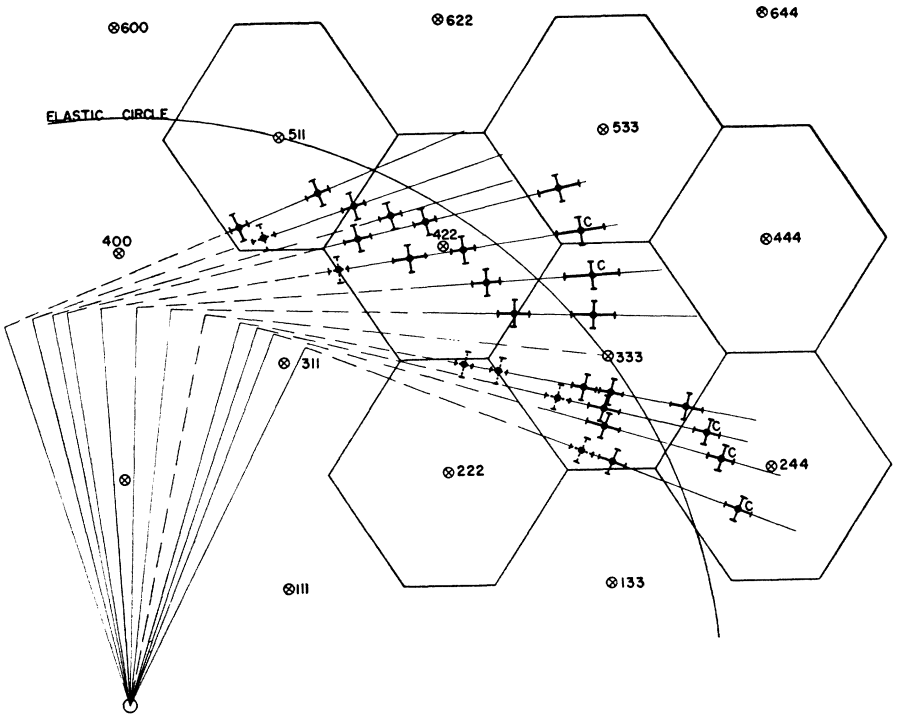

FIG. 6. The reciprocal lattice diagram for the $01\bar{1}$ plane of aluminum, with the results of experiment *A* in which incident neutrons of 0.0622 ev were employed at a scattering angle of 95.1°. The solid lines along **k'** indicate the range over which measurements were made.

of the areas of reciprocal space seen by the analyzing instrument while the inner lines represent the estimated half intensity contours.

The resolution can affect the results in two ways. It may be insufficient to resolve two distinct neturon groups which are then erroneously treated as one. Cases for which this is believed to have occurred are labeled "*c*." Or, because the intensity of the neutron groups can vary over the resolution function (indeed, the conservation equations may only be satisfied over part of the resolution function), the inferred position of a group may be altered from its true position by reason of the resolution. Neutron groups which are believed to be strongly affected by this effect are labeled "*d*."

(*a*) *Crystal Spectrometer Experiments*

A. The first experiments performed have been briefly reported.[8] Neutrons of incident wavelength 1.14_8 A (energy 0.062_2 ev) were scattered in reflection by the flat aluminum specimen through an angle of $\phi = 95.1°$, for which Bragg scattering by the 333 and 511 planes can occur. Measurements were made with the crystal in 11 different orientations in the $01\bar{1}$ plane. Typical distributions have been published.[8] These results, revised in some details since the preliminary publication, are shown in Fig. 6 on the reciprocal lattice diagram.

B. Using neutrons with the above wavelength two experiments were performed in which the scattering angle ϕ was altered to 88°. The results are shown in Fig. 5 on the reciprocal lattice diagram.

C. Neutrons of incident wavelength 1.523 A (energy 0.0351 ev) were scattered by the spherical single crystal through an angle of 98° at which Bragg scattering by the 400 planes can occur. Measurements were made with the crystal in 35 different orientations in the $01\bar{1}$ plane. Typical distributions are shown in Fig. 2(a). These results are plotted in Fig. 7 on the reciprocal lattice diagram.

Certain neutron groups were observed in the second order of the analyzing crystal and could be identified as such by both their positions and intensities. These groups are labeled "*b*." For our purposes they are contaminant groups. The two groups labeled "*a*" are believed to arise from contaminant second-order neutrons in the incident beam which have been Bragg scattered in the 355 reflection, and then observed in the second order of the analyzing crystal.

D. The regions of reciprocal space in the vicinity of certain reciprocal lattice points were studied under high resolution. The same conditions as experiment *C* were used except that an additional collimator of about 1.6° maximum angular acceptance was installed at position *C*1 in Fig. 1. Energy distributions at different orientations, 68°, 70°, 73°, 78°, 83°, 93°, 142°, 145°, and 148°, were obtained. Typical distributions are shown in Fig. 2(b). These results are included in the reciprocal lattice diagram of Fig. 7.

E. At the conclusion of the crystal spectrometer and filter chopper experiments it became apparent that more data were desirable in the simple directions 100, 111, and 110. In the meantime the crystal spectrometer

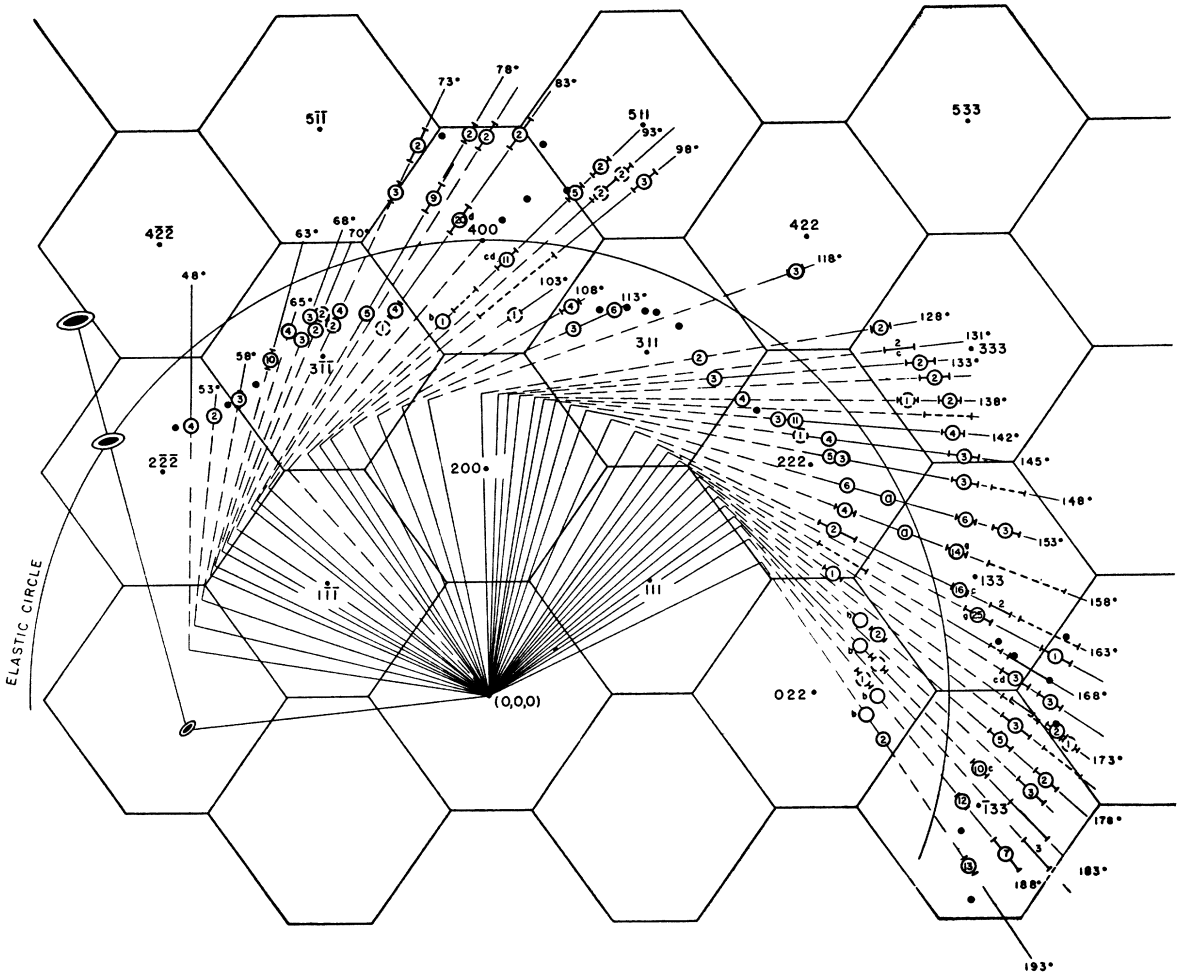

FIG. 7. The reciprocal lattice diagram for the $01\bar{1}$ plane of aluminum, with the results of experiments *C* and *D* in which neutrons of 0.0351 ev ($\lambda = 1.523$ A) were used at a scattering angle of 98°. The bars along $\mathbf{k}'$ indicate the full width at half-maximum of the observed neutron groups. The figures in the open circles give the corrected relative intensities of the groups. The closed circles are neutron groups reflected across the 100 or 011 directions. The symbols "*a*" and "*b*" indicate groups which are contaminant and symbols "*c*" and "*d*" groups whose position is somewhat uncertain as discussed in the text. Estimates of the area in reciprocal space covered by a neutron group are shown. The shaded inner figure is an estimate of the half-intensity contour of the neutron group.

had been modified in such a way that it was possible to adjust the angle of scattering ϕ conveniently and accurately.[13] Walker's results[11] and our accumulated neutron results gave a first approximation to $\nu(q)$ for the desired directions. The angle of scattering ϕ and the crystal orientation Ψ were then set so that a desired pair of values of ν and $\mathbf{q}$ would be obtained if the first approximation were correct. The remeasured values of ν and $\mathbf{q}$ gave a second approximation which could then be used as a basis for another measurement if required. In fact one measurement was almost always sufficient. Eight different measurements were made in the $01\bar{1}$ plane of the specimen crystal and fifteen measurements in the 100 plane, using neutrons of wavelength 1.529 A. The experimental arrangements were chosen in such a way that the resolution and intensity were especially favorable. The results of these experiments are distinguished on the succeeding figures (Figs. 11 to 13) by the letter "*e*."

(*b*) *Filter Chopper Experiments*

F. Using the filter chopper method with an angle of scattering of 90° and the spherical specimen, energy distributions were obtained for 36 orientations at intervals of 5° in the $01\bar{1}$ plane. Typical energy distributions are shown in Fig. 4. The results are presented in Fig. 8 on a reciprocal lattice diagram. The reciprocal lattice was covered twice with the resolution function differently oriented. The positions of all well-resolved neutron groups (open circles in the figure) were reflected through either the 100 or 011 symmetry axis of the diagram and are shown as small filled circles. The good agreement between directly observed and reflected groups is a check on the crystal alignment and indicates

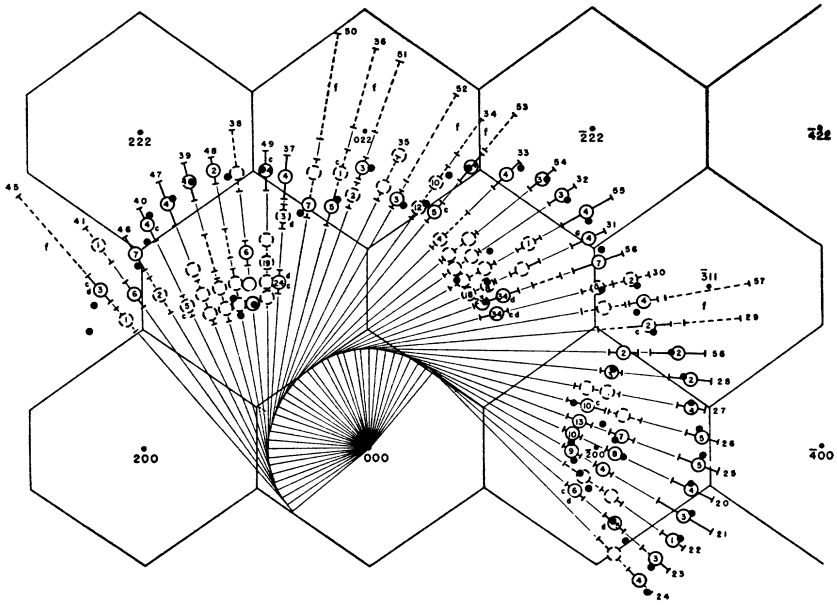

FIG. 8. The reciprocal lattice of the $01\bar{1}$ plane of aluminum with the results of experiment F in which the filter time-of-flight apparatus was used. The incident neutrons have a mean energy of 4.0×10^{-3} ev ($\lambda=4.55$ A) and the angles of scattering were about 90° as shown. The groups "c" and "d" have uncertainties in their position and the groups "f" are assigned to multiple phonon processes.

that in much of the data the effect of the resolution function is probably small.

G. Energy distributions were obtained at 18 orientations at 5° intervals in the 001 plane and are shown in Fig. 9 on the reciprocal lattice diagram. In this plane also the experiment covered twice the irreducible sector of the reciprocal lattice. All well-resolved neutron groups were again reflected into another region of the reciprocal lattice.

In both planes certain broad, weak neutron groups were observed which would yield implausibly large apparent ν and small apparent q. These groups, indicated by the symbol f in Figs. 8 and 9, are believed to have been produced by a double phonon process in which two phonons were annihilated.[17]

2. Experimental Dispersion Curves $\nu_j(q)$

By reason of crystal symmetry the $\mathbf{q}$'s obtained in the $01\bar{1}$ plane by joining the neutron group positions to the nearest reciprocal lattice point can be plotted in one-quarter of a reduced zone as shown in Fig. 10(a). This reduced zone has been divided into eleven different sectors of 9° full width. The neutron groups of Figs. 5 to 8 have been assigned to their appropriate sectors. The direction of $\mathbf{q}$ is henceforth taken as the direction of the center of the sector. The frequency ν of the phonon was determined from Eq. (2b) and plotted (Fig. 11) against the wave number $q/2\pi$ for the eleven sectors. The errors have been assigned by a convention that the possible misplacement of a neutron group is about one quarter the observed full width at half-maximum of the group. These errors are thought to correspond roughly to standard deviations. The

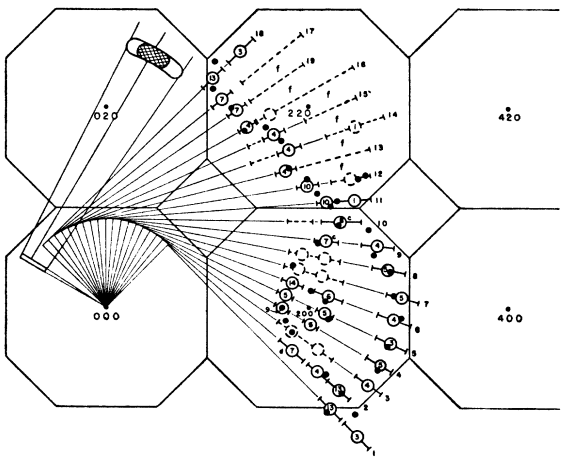

FIG. 9. The reciprocal lattice diagram of the 001 plane of aluminum and the results of experiment G in which neutrons of the incident energy $E=4.0\times10^{-3}$ ev ($\lambda=4.55$ A) were used. The approximate limits of the resolution function in reciprocal space are indicated as well as the half-intensity contour as before.

[17] The total cross section for double phonon annihilation is roughly 10% of the cross section for single phonon annihilation, estimated following G. L. Squires [Proc. Roy. Soc. (London) **A212**, 192 (1952)]. The apparent frequencies of the groups f are about 8 to 12×10^{12} cps. The frequency distribution for aluminum as calculated by Walker (Figs. 5, 6, reference 11) shows that about 40% of the frequency distribution consists of essentially transverse modes with frequencies 4 to 6×10^{12} cps. The total double phonon scattering will thus show a broad peak in the range 8 to 12×10^{12} cps. The scattering with this apparent frequency will occur in regions of the reciprocal lattice for which the polarization and Jacobian factors in the equivalent of Eq. (4) for the double phonon process are favorable. The polarization factor is most favorable when the neutron group is in the region of a reciprocal lattice point since the two modes involved are both approximately transverse and of large wave number. The Jacobian factor is favorable when an increase in the two q's results in an increase in ν for both phonons and therefore for the apparent ν—that is when the neutron group lies outside the reciprocal lattice point. Thus the double phonon groups are expected in the positions in which they are actually observed.

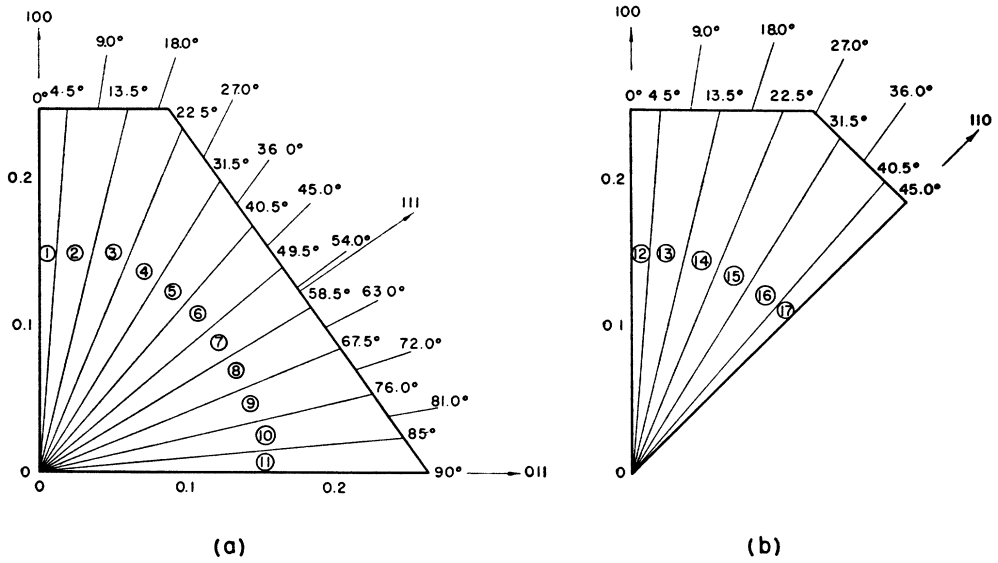

FIG. 10. The irreducible zone sectors in (a) the $01\bar{1}$ plane and (b) the 001 plane, and the 9° sectors into which they are divided. The circled numerals identify the direction of the dispersion relations shown in Figs. 11 and 12.

meanings of the different symbols are given in the inset. It will be observed that the results for the three different incoming energies, for neutron energy gain (phonon annihilation) or loss (phonon creation), and for the two instrumental methods appear consistent.

Similarly the q's obtained in the 001 plane (Fig. 9 and experiment E) have been plotted in six sectors of one-eighth of a reduced zone as delineated in Fig. 10(b). The frequencies are plotted as functions of the wave number $q/2\pi$ in Fig. 12. Two of the sector directions (of the type 100 and 110) also appear in the $01\bar{1}$ plane (Fig. 11).

In Figs. 11 and 12 the points which were obtained in experiment E have been identified with the symbol "e."

IV. DISCUSSION

1. The Scattering Curves

The neutron groups of Figs. 6 to 9 fall on curves (not shown) that can often be traced for considerable distances. These curves are sections of scattering surfaces, similar to those discussed by Placzek and Van Hove[4] and by Lowde.[18] Placzek and Van Hove have shown that there are in general at least three such scattering surfaces, one for each branch of the frequency spectrum and that for every vector direction $\mathbf{k}'/|\mathbf{k}'|$ there are at least three solutions of Eqs. (2) which result in neutron groups. Computations of scattering surfaces using particular models of atomic forces have been made by Squires[19] for aluminum and by Sjolander[20] for potassium chloride.

The 100 and $01\bar{1}$ planes of a face-centered-cubic lattice are both planes of reflection symmetry. For such mirror planes symmetry requires that two branches of the frequency spectrum have their polarization vectors in the plane and that one branch has its polarization vector normal to that plane.[21] Since only the component of the polarization vector along $\mathbf{k}-\mathbf{k}'$ is effective in scattering [Eq. (4)] the intensity of the branch with polarization normal to the plane is identically zero. Thus only two branches can appear in these scattering diagrams and in fact only two have been observed.

The variations of intensity of the neutron groups can also be qualitatively understood. The cross sections of Weinstock[22] for annihilation or creation of one phonon have been summed (by Waller and Froman[4]) over the number of normal modes involved in one neutron group [i.e., the number which can simultaneously satisfy Eqs. (2)] with the result

$$\sigma_j(\mathbf{k}\to\mathbf{k}')=\frac{\sigma_{\mathrm{coh}}}{4\pi M}\frac{k'}{k}\begin{Bmatrix}N_\lambda\\ N_\lambda+1\end{Bmatrix}\frac{e^{-2W}}{\nu}\frac{[(\mathbf{k}-\mathbf{k}')\cdot\boldsymbol{\alpha}_j]^2}{|J_j|} \quad (4)$$

per 4π steradians per nucleus. σ_{coh} is the coherent scattering cross section of the scattering nucleus, M is the mass of the nucleus and e^{-2W} is the Debye-Waller factor. For phonon annihilation (neutron gain of energy) $N_\lambda=[\exp(h\nu/k_BT)-1]^{-1}$ is used; for phonon creation (neutron loss of energy) $N_\lambda+1$ is used. The factor $J_j=1+(\epsilon h/2E')[\mathbf{k}'\cdot\mathrm{grad}_q\nu_j]$ where $\epsilon=+1$ for neutron energy loss and -1 for neutron energy gain.

The reciprocal lattice diagrams, show that the intensities are largest near the reciprocal lattice points as required by Eq. (4) which gives intensities proportional to ν^{-2} for small ν. The factor $[(\mathbf{k}-\mathbf{k}')\cdot\boldsymbol{\alpha}_j]^2$

[18] R. D. Lowde, Proc. Roy. Soc. (London) **A221**, 206 (1954).
[19] G. L. Squires, Phys. Rev. **103**, 304 (1956).
[20] A. Sjolander (unpublished).

[21] The theorem is proved as follows. The mutually perpendicular polarization vectors $\boldsymbol{\alpha}_j(\mathbf{q})$ must be continuous functions across the mirror plane. For $\mathbf{q}$ in the mirror plane this is possible only if $\boldsymbol{\alpha}_j$ is either normal to the plane or in it, as may be seen by considering a vector $\mathbf{q}$ slightly out of the plane.
[22] Reference 3, Eq. (36).

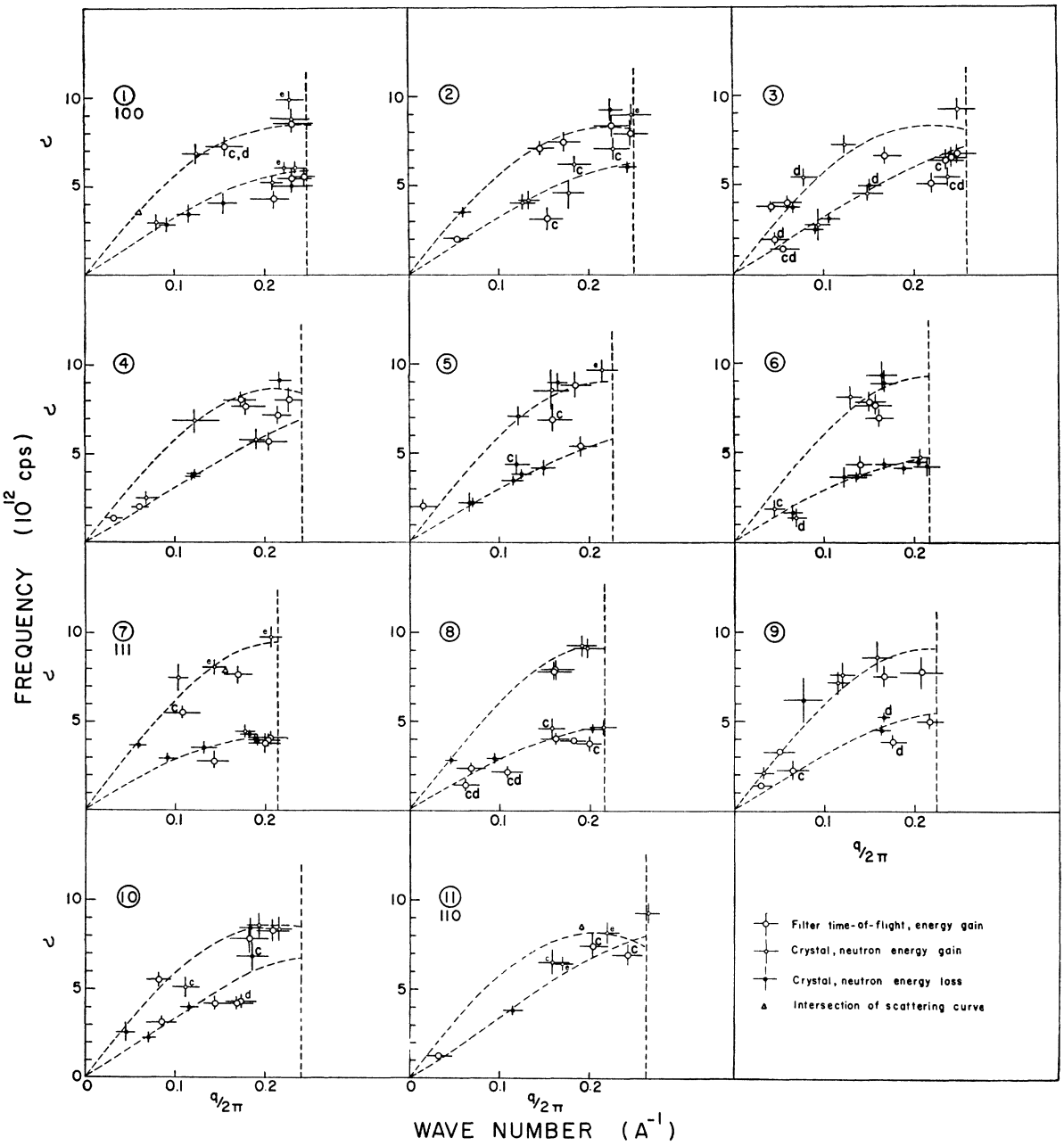

FIG. 11. The frequency-wave number curves for the eleven sector directions in the $01\bar{1}$ plane. Points labeled "*c*" and "*d*" are expected to be more than usually uncertain in position as discussed in the text. Those labeled "*e*" were obtained in experiment *E*. The dashed curves are the calculated nine constant dispersion curves of Walker. The circled numerals refer to the sectors of Fig. 10.

has been mentioned earlier. For small ν the polarization vectors $\boldsymbol{\alpha}_j$ are nearly perpendicular (transverse waves) or parallel (longitudinal waves) to $\mathbf{q}$ because of the isotropic elasticity of the aluminum crystal. Referring to Fig. 7 in the region of the $3\bar{1}\bar{1}$ lattice point, the intensity of the principal scattering curve is seen to decrease as $\mathbf{q}$ becomes parallel to $\mathbf{k}-\mathbf{k}'$. At the same time a higher energy scattering curve closer to the reciprocal lattice point appears. The two curves are clearly due to transverse and longitudinal waves, respectively. The same phenomenon is visible in other sections of the reciprocal lattice diagram.

The factor $|J_j|^{-1}$ measures the relative number of normal modes which can contribute to a neutron group. It can influence the intensity strongly as can be seen for example by comparing the intensity of the two

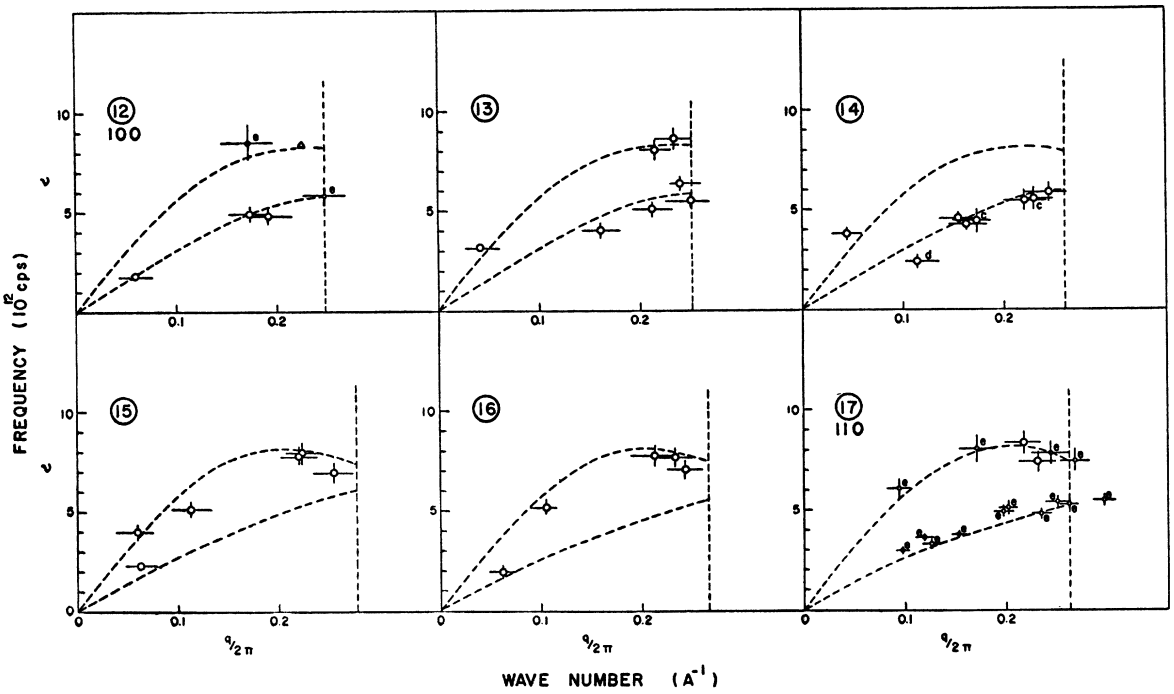

FIG. 12. The frequency-wave number curves for the six sector directions in the 001 plane. See the caption of Fig. 11. The sectors marked 12 and 17 are in the same directions as the sectors marked 1 and 11 in Fig. 11.

phonons marked "g" in the 133 zone of Fig. 7. The group for which $\mathbf{k}'\cdot\mathrm{grad}_q\nu_j$ is negative is more intense although its frequency is the higher of the two.

2. Dispersion Relations and the Interatomic Forces

For the simple directions of types 100, 111, and 110 the waves are either strictly transverse or longitudinal because of symmetry. The two transverse branches are degenerate in the 100 and 111 directions. In the 011 direction the polarizations of the transverse branches are in the $01\bar{1}$ and 100 directions. The first takes part in neutron scattering in the 100 plane, the second in the $01\bar{1}$ plane. In other directions in the mirror planes only one of the two transverse branches takes part in scattering as has been seen.

In Figs. 11 and 12 the results are compared with the appropriate branches of dispersion curves of Walker[11] which he obtained by fitting a nine constant secular equation (general forces out to third neighbors) to his measurements of x-ray intensities in the simple directions of types 100, 111, and 110. The agreement between the neutron results and Walker's nine constant calculated curves (shown as dashed lines) is on the whole good, although some deviations seem to occur.

It would be possible to fit the nine-constant secular equation anew to the results of both experiments and thus obtain an improved set of force constants. This This would require least squares fitting of the quadratic secular equations[23] to the data. However the improvement in the force constants would probably not be great, and it has seemed to us better to take a more physical approach to the analysis.

The applicability of the Born-Von Karman theory to metals is perhaps doubtful because there are terms in the binding energy which do not arise simply from interactions between ions. Thus even if a good fit is obtained using the Born lattice dynamics the meaning to be attached to the force constants is not clear. Fuchs[24] has shown that for some monovalent metals it is a good approximation to consider the energy as consisting of terms dependent only on the volume plus interactions between ions. DeLaunay[25] and Bhatia[26] have used this idea to compute dispersion curves for simple models of metals. In these models the transverse branches in the simple directions are unaffected by the volume dependent terms. Leigh[27] has made calculations of elastic constants for the trivalent metal aluminum, and has found additional complicating effects. Unfortunately we have been unable to apply his results to the problem of lattice frequencies. The results of

[23] In the simple directions the cubic secular equation[11] factors into three linear equations. In the mirror planes the secular equation factors into a linear equation and a quadratic. The polarization vectors of the modes corresponding to the linear equation are perpendicular to the mirror plane and do not contribute to the neutron results.

[24] K. Fuchs, Proc. Roy. Soc. (London) **A153**, 622 (1935); **A157**, 444 (1936).

[25] J. DeLaunay, J. Chem. Phys. **21**, 1957 (1953).

[26] A. B. Bhatia, Phys. Rev. **97**, 363 (1955).

[27] R. S. Leigh, Phil. Mag. **42**, 139 (1951).

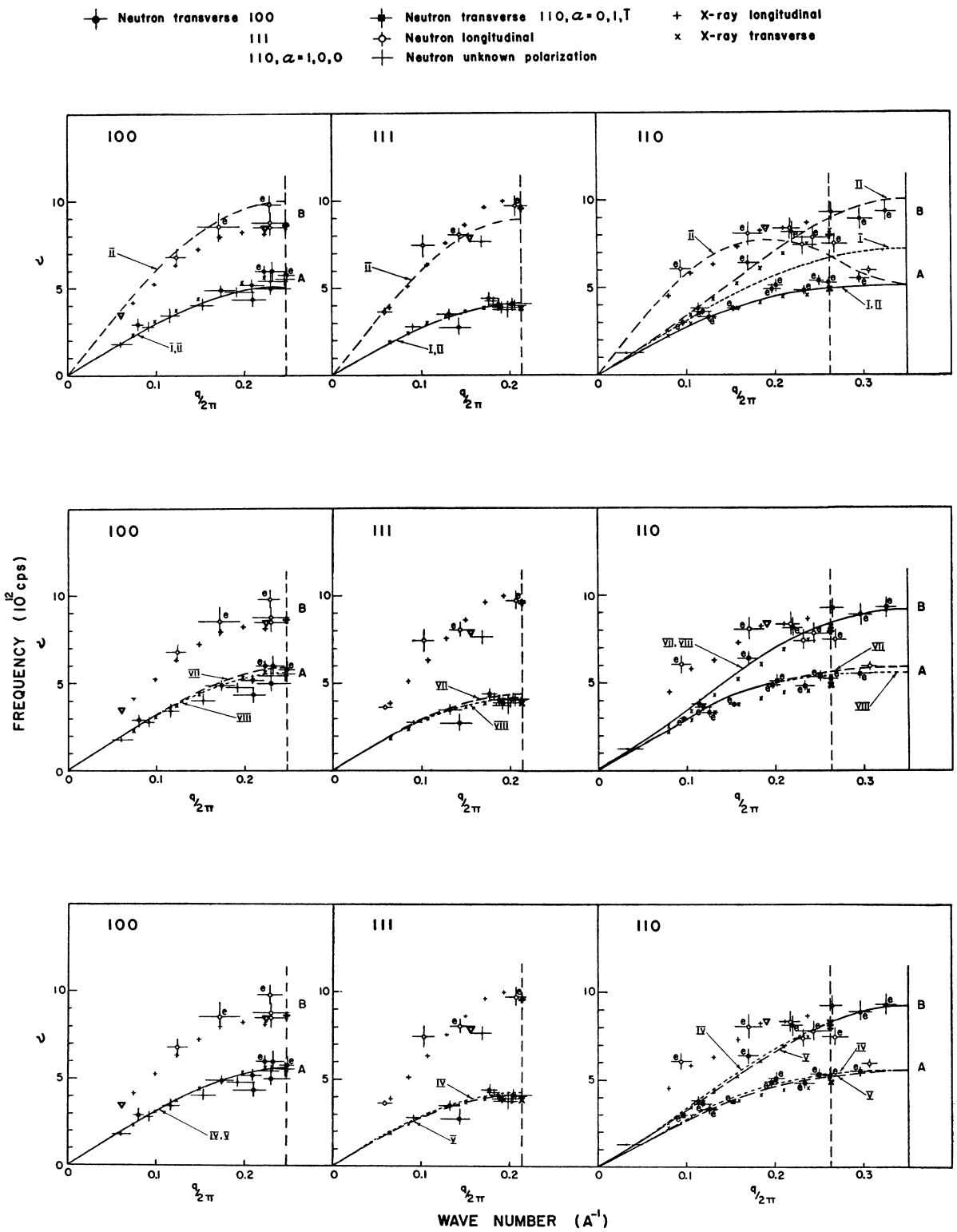

FIG. 13. The frequency-wave number relations for the three special directions. Points labeled "*c*" or "*d*" in Figs. 11 and 12 have been omitted. The curves are best fits of various simple models as given in Tables I and II.

TABLE I. Models[a] used in fitting the dispersion curves and the elastic constants.

Model[a]	Type of force	Neighbor	Constants	Comments
I	C	1 2	θ_1 θ_2	no fit [Fig. 13(a)]
II	NC	1	α_1 β_1 γ_1	no fit [Fig. 13(a)]
III	NC	1	α_1 β_1 γ_1	no fit
IV	NC	1	α_1 β_1 $(\gamma_1-\alpha_2)$	probably no fit [Fig. 13(c)]
	C	2 3	θ_3	
V	NC	1 2	α_1 β_1 $(\gamma_1-\alpha_2)$ β_2	probably fit [Fig. 13(c)]
VI	NC	1 2	α_1 β_1 $(\gamma_1-\alpha_2)$ β_2	fit
	C	3	θ_3	
VII	C	1 2 3	θ_1 θ_2 θ_3	probably no fit [Fig. 13(b)]
VIII	C	1 2 3 4	θ_1 θ_2 θ_3 θ_4	probably no fit [Fig. 13(b)]

[a] Model I was fitted to the two shear elastic constants alone, c_{44} and $(c_{11}-c_{12})/2$. Model II was fitted to the three elastic constants c_{11}, c_{12}, and c_{44}. All other models were fitted to the two shear elastic constants c_{44} and $(c_{11}-c_{12})/2$ and to the dispersion curves for the transverse modes in the three simple directions.

deLaunay and of Bhatia suggest that some of the difficulties associated with the influence of the conduction electrons on the lattice frequencies may be avoided by restricting consideration to the transverse modes. Force constants so obtained may have more physical significance than force constants obtained by fitting all the lattice waves.

We have proceeded in this way, fitting the measurements of the strictly transverse waves in the simple directions with the results of calculations for some simple models. The experimental results for the simple directions are replotted in Fig. 13, dropping the uncertain points labeled "*c*" and "*d*." Different symbols indicate the polarization where this could be definitely established from the intensities. Walker's x-ray results are also given in Fig. 13. In comparing the x-ray and neutron results and estimating errors it should be realized that the errors involved in the x-ray measurements are largely systematic and whill be expected to change the various curves as a whole rather than the relation of adjacent points. The neutron errors are probably almost random, except for the lower transverse curve in the 110 direction which depends solely on experiment *E* and hence possibly includes a systematic error.

Several models were fitted by least squares to the experimental results as shown in Table I. In this table "C" and "NC" refer to central and noncentral forces, respectively, and the numerals in the "neighbors" column specify the shells of neighbors. In one model (II) the three elastic constants[28] only were used to determine the three atomic constants (first neighbor noncentral) of the model. In the other models only the shear elastic constants (c_{44}, $(c_{11}-c_{12})/2$) were used together with (except I) the neutron and x-ray dispersion results for the transverse modes in the simple directions. The secular equation for determining the frequencies as a function of the force constants was that used by Walker.[11] Extension of the secular equation to fourth neighbors was easily made since these have the same symmetry as first neighbors. Definitions of the force constants for the various models are given in Table II. In the least squares fitting the neutron and x-ray results were given about equal weight. The total weight of the dispersion relation data was taken to be slightly less than the weight of each of the elastic constants. The input data for the 110 direction and the weights assigned to the elastic constants were varied. Some forty fits were made. Choice of the higher (or lower) data in the 110 direction seemed only to increase (or decrease) the scale of the derived force constants. If the x-ray and neutron results are given equal weights in the 110 direction (as in the 111 and 100 directions)

TABLE II. Interatomic force constants in units of 10^4 dynes/cm, obtained by least squares fitting of the models of Table I to the neutron and x-ray dispersion curves and to the elastic constants.[a]

Force constant	Model I	II	III	IV	V	VI	VII	VIII
$\alpha_1=D(101)_{11}$		1.105	0.955	0.969	0.956	0.962		
$\beta_1=D(101)_{22}$	$\theta_1=1.148$	−0.530	−0.362	−0.150	−0.1256	−0.202	$\theta_1=1.92$	$\theta_1=1.96$
$\gamma_1=D(101)_{13}$		0.934	0.796	$(\gamma_1-\alpha_2)=0.808$	$(\gamma_1-\alpha_2)=0.790$	$(\gamma_1-\alpha_2)=0.794$		
$\alpha_2=D(200)_{11}$					−0.062	−0.035		
$\beta_2=D(200)_{22}$	$\theta_2=0.169$						$\theta_2=0.16$	$\theta_2=0.164$
$\alpha_3=D(211)_{11}$								
$\beta_3=D(211)_{22}$								
$\gamma_3=D(211)_{23}$				$\theta_3=-0.081$		$\theta_3=-0.038$	$\theta_3=-0.130$	$\theta_3=-0.173$
$\delta_3=D(211)_{12}$								
$\alpha_4=D(202)_{11}$								
$\beta_4=D(202)_{22}$								$\theta_4=0.059$
$\gamma_4=D(202)_{13}$								

[a] Notes: 1. The force constant $D(hkl)_{ij}$ is the force in direction i on the atom at the origin due to a unit displacement in direction j of the atom at position $(hkl)a/2$. 2. The subscripts of the α_i, β_i, θ_i, etc., indicate the shell of neighbors. 3. The central force constant θ_i is the force on the atom at the origin along the line of centers of two atoms due to a motion of an atom of shell i along the line of centers. For central forces $\theta_1=2\alpha_1=2\gamma_1$; $\beta_1=0$: $\theta_2=\alpha_2$; $\beta_2=0$: $\theta_3=3\alpha_3/2=3\delta_3=6\gamma_3=6\beta_3$: $\theta_4=2\alpha_4=2\gamma_4$; $\beta_4=0$.

[28] The average values of the elastic constants of the authors of reference 10 as given by Squires[19] were used, *viz.*, $c_{11}=1.092\times10^{12}$, $c_{12}=0.640\times10^{12}$, and $c_{44}=0.284\times10^{12}$ dynes/cm^2.

the force constants listed in Table II are obtained for the various models.

A selection of the fits obtained with some of the models are shown in Fig. 13. Model I is equivalent to the models used by DeLaunay and Bhatia. The lack of fit excludes their special models but not the general philosophy on which they were based. The force constants obtained for the central force models (VII and VIII) have signs which imply potentials of peculiar shape which may be evidence against these models. Central force models with more than four interacting shells of neighbors would probably fit the data accurately and might overcome this objection. Models with noncentral forces and first neighbors only (II, III) do not fit. Introduction of a second neighbor central force constant $\alpha_2=\theta_2$ does not help because the constants γ_1 and α_2 always enter the transverse modes as the linear combination $\gamma_1-\alpha_2$. Introduction of a third neighbor central force constant (IV) improves the fit but does not eliminate discrepancies. Introduction of a second neighbor noncentral constant (V) probably allows a fit, although a small third neighbor central force constant (VI) improves it slightly.

In all central force models the second neighbor constant θ_2 turned out to be positive. In all noncentral force models $\alpha_1>\gamma_1-\alpha_2$, $\beta_1<0$, and $\beta_2<0$. For the noncentral models the constant α_2 must be determined from the longitudinal modes or the data in other directions.

Relatively complicated models are necessary to fit even the data for the transverse branches in the simple directions. Addition of other constants may be necessary to obtain a complete fit to all branches.[29]

V. CONCLUSIONS

This paper has presented measurements of the $\nu(\mathbf{q})$ dispersion relation in the two mirror planes (of type 110 and 100) of aluminum. The results agree fairly well with the dispersion relations obtained from x-ray intensity measurements by Walker for the three most symmetric directions, and with his nine-constant calculated dispersion curves for other directions. In an attempt to isolate the ionic core force constants, a number of models have been fitted to the purely transverse waves in the three symmetry directions. It has been shown that relatively complex models are required to fit even these limited data, and considerable information about possible models of the interatomic forces has been obtained. Further analysis utilizing all the data should yield additional information. The results presented, although still inadequate in terms of the problem, show very definitely the potentialities of these types of experiment.

The method of neutron spectrometry has the outstanding virtue that no theoretical or experimental corrections to the measurements are required, in contrast to the method of determination of the dispersion curves by x-ray intensity measurements, in which important corrections[11] for Compton scattering[30] and multiple phonon scattering must be applied. Furthermore the x-ray intensity measurements outside the symmetry directions are not readily interpretable in terms of dispersion curves, while neutron measurements will give the dispersion relations in all directions. At the present time, however, the x-ray technique has the considerable advantage of higher intensity and better resolution in reciprocal space.

The two methods for the neutron measurements which are described in this paper are to a considerable extent complementary. The crystal spectrometer method suffers from a comparatively low intensity and from the fact that rather large values of $\mathbf{k}$ and $\mathbf{k}'$ are used, thus necessitating accurate specimen crystal alignment. The simplicity, flexibility, and convenience of operation are strong points in its favor. The filter-chopper method is more favorable from the intensity point of view and because of the small values of $\mathbf{k}$ and $\mathbf{k}'$ the crystal alignment problem is minimized. The resolution is inherently limited by the small choice of filter materials available. Improvement in the resolution could be secured by replacing the lead subtraction filter by a beryllium oxide filter whose limiting wavelength is closer to that of beryllium than is the limiting wavelength of lead. However because the intensities of the two patterns to be subtracted would be comparable the counting time would be much longer. Systems using other types of energy defining elements are also feasible. The choice of the best system depends upon the type of experiment to be performed.

As the experiments improve it can be expected that data accurate enough to establish the general features of the atomic force fields in crystals will be obtained. Already the data are able to exert a considerable degree of selection over possible models. It would assist greatly in future work if there were available general theories more directly adapted to metals than the Born-Von Karman theory, to serve as a frame in analyzing the results. Such general theories would be useful even though they contained a considerable number of undetermined parameters.

ACKNOWLEDGMENTS

The authors are indebted to Dr. G. H. Goldschmidt, Dr. D. G. Hurst, and Dr. N. K. Pope for a conversation in 1950 which led to the design of these experiments, and to Dr. Hurst and Dr. Pope for many discussions since. We thank Dr. J. M. Kennedy for the least square fits made on the Chalk River Datatron, and Mr. G. R. DeMille, Mr. R. S. Weaver, Mrs. J. M. Denovan, and Mr. R. A. Fraser for assistance in the experiments and in the analysis.

[29] *Note added in proof.*—One constant is necessary to fit the elastic constant C_{11} and probably at least one other to fit the remaining neutron and x-ray data. Thus clearly the use of at least six constants in a properly chosen model is indicated.

[30] H. Curien, Revs. Modern Phys. **30**, 232 (1958), this issue.